Automatica 160 (2024) 111444

Contents lists available at ScienceDirect

Automatica

journal homepage: www.elsevier.com/locate/automatica

Brief paper

Rolling self-triggered distributed MPC for dynamically coupled nonlinear systems☆

Tao Wang [a,b], Yu Kang [b,c,*], Pengfei Li [b,**], Yun-Bo Zhao [b], Hao Tang [a]

[a] Department of Automation, Hefei University of Technology, Hefei, 230009, China
[b] Department of Automation, University of Science and Technology of China, Hefei, 230027, China
[c] Institute of Advanced Technology, University of Science and Technology of China, Hefei, 230000, China

ARTICLE INFO

Article history:
Received 5 July 2022
Received in revised form 16 October 2023
Accepted 6 November 2023
Available online xxxx

Keywords:
Dynamically coupled systems
Distributed model predictive control
Self-triggered control
Constrained nonlinear systems

ABSTRACT

The mutual influences caused by dynamic couplings in large-scale systems increase the difficulty in the design and analysis of distributed model predictive control (DMPC), and require information exchange among subsystems which calls for a scheduling strategy to save communication resources in communication-limited environments. To circumvent the two problems, we design a rolling self-triggered DMPC strategy for large-scale dynamically coupled systems with state and control input constraints. First, the optimal control problem where the cost is subject to the coupled dynamic and the constraints are subject to the uncoupled counterpart is proposed, forming the dual-model DMPC that is simple in design and analysis but yields good control performance. Second, the information exchange only occurs at some specified triggering instants determined by a rolling self-triggered mechanism, saving communication resources more significantly. The effectiveness of the designed strategy is verified by numerical simulations.

1. Introduction

Many practical systems, such as hydropower plants (Hanmandlu & Goyal, 2008), urban traffic (Eini & Abdelwahed, 2019), and supply chains (Fu, Zhang, Dutta, & Chen, 2019), are large-scale systems and can be formulated by nonlinear dynamics consisting of several dynamically coupled subsystems. For such large-scale systems, it is often impossible to implement a centralized control strategy. Even if such a centralized control strategy can be implemented, the resultant high computational complexity renders it impractical (Antonelli, 2013). Therefore, for such large-scale systems, a distributed counterpart is often employed because it reduces computational complexity by distributing decisions based on all subsystems (Dunbar, 2007). Moreover, constraints, i.e., physical limits, system safety, and desired performance, often exist in practical systems. In this context, the desired control strategy should have a distributed control structure and can handle constraints.

Distributed model predictive control (DMPC), which can handle constraints, has found wide applications in large-scale coupled systems, see, for example, Alessio, Barcelli, and Bemporad (2011), Dunbar (2007), Hans, Braun, Raisch, Grüne, and Reincke-Collon (2018), Jia and Krogh (2002), Liu, Abbas, and Velni (2018), Liu, Shi, and Constantinescu (2014), Ma, Liu, Zhang, and Xia (2020), Magni and Scattolini (2006) and Shalmani, Rahmani, and Bigdeli (2020). Studies can be classified into two categories according to how they deal with mutual influences between subsystems caused by dynamic couplings.

In the first category, coupling terms are treated as external disturbances (Alessio et al., 2011; Jia & Krogh, 2002; Liu et al., 2014; Magni & Scattolini, 2006). For example, the works in Alessio et al. (2011), Liu et al. (2014) and Magni and Scattolini (2006) ignore mutual influences in the predictive model of each subsystem, and the analysis is conducted by using the upper bound of mutual influences. While in Jia and Krogh (2002), mutual influences are viewed as the disturbances in the predictive model, and a min–max feedback DMPC strategy is investigated. In general, the design and analysis methods of the DMPC strategy in this category are simple, as they can be borrowed from those in conventional centralized MPC for perturbed systems. However,

☆ This work was supported in part by the National Key Research and Development Program of China under Grant 2018AAA0100801, in part by the National Natural Science Foundation of China under Grant 62103394, Grant 62173317, Grant 62033012, and Grant 62273130, and in part by the Science and Technology Major Project of Anhui Province (202104a05020064). The material in this paper was not presented at any conference. This paper was recommended for publication in revised form by Associate Editor Marcello Farina under the direction of Editor Ian R. Petersen.

* Corresponding author at: Department of Automation, University of Science and Technology of China, Hefei, 230027, China.
** Corresponding author.
E-mail addresses: wanghtao@mail.ustc.edu.cn (T. Wang), kangduyu@ustc.edu.cn (Y. Kang), puffylee@ustc.edu.cn (P. Li), ybzhao@ustc.edu.cn (Y.-B. Zhao), htang@hfut.edu.cn (H. Tang).

https://doi.org/10.1016/j.automatica.2023.111444
0005-1098/

the predictive model in the optimal control problem (OCP) is inaccurate, resulting in poor control performance (Ma, Liu, Zhang, & Xia, 2020; Shalmani et al., 2020).

In the second category, the coupling terms in each subsystem, which are predicted by using the information transmitted from other subsystems via communication networks, are exploited in the predictive model. In this context, many different DMPC strategies for large-scale coupled systems are investigated, see, e.g., the robust non-iterative DMPC strategy in Ma, Liu, Zhang, and Xia (2020), the iterative Nash-based robust DMPC strategy in Shalmani et al. (2020), and the distributed receding horizon control strategy in Dunbar (2007). It is noteworthy that the utilization of the information from other subsystems in this category helps to improve the prediction precision, thereby obtaining better control performance. Nevertheless, the coupling terms in the predictive model complicate the analysis of the feasibility of the OCP and the stability of the overall systems. To be specific, to guarantee feasibility and stability, some extra constraints (Dunbar, 2007; Ma, Liu, Zhang, & Xia, 2020), e.g., consistency constraint (Dunbar, 2007), and some auxiliary parameters that should satisfy stringent equality and inequality conditions, are added in the OCP, which increases the design complexity. Moreover, the required periodic information exchange among subsystems occupies communication resources, which may be not affordable in communication-limited environments.

To save communication resources, a promising approach is to incorporate DMPC with an event- or self-triggered mechanism (Berkel & Liu, 2018; Eqtami, Heshmati-Alamdari, Dimarogonas, & Kyriakopoulos, 2013; Hashimoto, Adachi, & Dimarogonas, 2014; Kang, Wang, Li, Xu, & Zhao, 2022; Liu, Li, Shi, & Xu, 2020; Ma, Liu, Zhang, Liu, & Xia, 2020; Zhou, Li, Xi, & Gao, 2022). In this way, the OCP is solved and the information among subsystems is exchanged only when some prescribed conditions are met. In event-triggered DMPC, states are continuously sampled to check whether the event is triggered. Related works on event-triggered DMPC for coupled systems can be found in Berkel and Liu (2018), Kang et al. (2022), Liu et al. (2020), Ma, Liu, Zhang, Liu, and Xia (2020) and Zhou et al. (2022). For coupled linear systems, event-triggered DMPC with a fixed prediction horizon (Berkel & Liu, 2018; Zhou et al., 2022), and an event-triggered DMPC scheme with an adaptive prediction horizon (Ma, Liu, Zhang, Liu, & Xia, 2020) are proposed. For coupled nonlinear systems, a novel distributed event-triggered strategy and a compound event-triggered DMPC strategy are developed in Kang et al. (2022) and Liu et al. (2020), respectively. To overcome the drawback of continuous sampling in event-triggered DMPC, self-triggered DMPC is investigated (Eqtami et al., 2013; Hashimoto et al., 2014), where the next triggering instant is precomputed based on the subsystem model as well as the latest predictive control input and/or state information. However, the estimation of future system behavior is susceptible to disturbances, leading to more conservative triggering results compared with event-triggered DMPC. Furthermore, studies on self-triggered DMPC for coupled systems have not been reported due to the difficulty in evaluating the variation of the mutual influences between two consecutive triggering instants.

In this paper, our task is to design an efficient self-triggered DMPC strategy for large-scale coupled nonlinear systems. In light of the above discussion, this task faces two challenges.

(a) How to obtain a DMPC strategy that is easy-to-design and has good control performance? Note that the DMPC strategy in the first category is simple in design but yields poor performance, while the one in the second category is just the opposite. Therefore, the existing DMPC strategies in both categories fail to solve this challenge.

(b) How to design an efficient self-triggered mechanism that bypasses the evaluation of the variation induced by mutual influences? Note that incorporating the conventional self-triggered mechanism, see, e.g., Eqtami et al. (2013), Hashimoto et al. (2014) and Sun, Dai, Liu, Dimarogonas, and Xia (2019), with the DMPC in the first category is fairly conservative as only the worst-case mutual influences are considered. Moreover, combining the conventional self-triggered mechanism with the DMPC in the second category is also not the ideal candidate as obtaining an accurate prediction of this variation is an intractable task.

In this paper, we propose a novel OCP, which inherits both the advantages from the above two categories, to solve the first challenge, and improve the self-triggered mechanism which is first proposed in our conference paper (Wang, Li, Kang, & Zhao, 2021), to handle the second challenge.

The main novelties and contributions are as follows.

- A dual-model OCP is designed, which is simple in design and yields desirable control performance. Specifically, this OCP consists of both the coupled model and the decoupled model, where the coupled model is employed to improve control performance and the decoupled model facilitates the design of the constraints and parameters to ensure recursive feasibility and stability.
- A rolling self-triggered mechanism is developed, which saves communication resources more efficiently. In this mechanism, the states may be sampled several times between two consecutive triggering instants and the sampling instants are determined by using the conventional self-triggered mechanism in a rolling manner. Based on the sampled states, the actual state predictive error can be obtained, and the accurate evaluation of the mutual influences is no longer a strict requirement.
- Sufficient conditions for recursive feasibility and stability are established, which are much simpler and easier to be satisfied than those obtained by the DMPC strategy in the aforementioned second category. This benefit is also a positive effect induced by the dual-model OCP.

Notations. Let $\mathbb{Z}$ and $\mathbb{N}$ denote the nonnegative integers and positive integers. The symbols $\mathbb{R}$ and $\mathbb{R}^n$ represent real numbers set and n-dimensional real space. For a symmetric matrix P, $P \succ 0$ means that P is a positive matrix. For a vector $x \in \mathbb{R}^n$, x^T, $\|x\| = \sqrt{x^T x}$, and $\|x\|_P$ with $P \succ 0$ denote its transpose, Euclidean norm and P-weighted norm, respectively. For matrix $P \in \mathbb{R}^{n\times n}$, its maximum and minimum eigenvalue are $\lambda_{\max}(P)$ and $\lambda_{\min}(P)$, respectively. Given two nonempty sets $\mathbb{X}$ and $\mathbb{Y}$, $\mathbb{X} \oplus \mathbb{Y} \triangleq \{x+y | x \in \mathbb{X}, y \in \mathbb{Y}\}$ represents the Minkowski addition set, and $\mathbb{X} \ominus \mathbb{Y} \triangleq \{x : x+y \in \mathbb{X}, \forall y \in \mathbb{Y}\}$ represents the Pontryagin difference set. Diag{...} denotes a block-diagonal matrix.

2. Problem formulation and preliminaries

2.1. Problem formulation

Consider a large-scale system consisting of M nonlinear interconnected subsystems, which are coupled through states. The dynamical coupling between subsystems is described by a directed graph $\mathcal{G} = (\mathcal{M}, \mathcal{E})$, where $\mathcal{M} = \{1, \ldots, M\}$ is the set of nodes (subsystems) and $\mathcal{E} \subset \mathcal{M} \times \mathcal{M}$ is the set of edges. The dynamics of ith subsystem is given by

$$\dot{x}_i(t) = f_i(x_i(t), u_i(t)) + \sum_{j\in\mathcal{N}_i^u} g_{ij}(x_j(t)) + w_i(t), t \geq 0, \quad (1)$$

where $i \in \mathcal{M}$, $x_i(t) \in \mathbb{R}^{n_i}$ and $u_i(t) \in \mathbb{R}^{m_i}$ are state and control input respectively, and they are constrained by

$$x_i(t) \in \mathcal{X}_i, u_i(t) \in \mathcal{U}_i. \tag{2}$$

The sets $\mathcal{X}_i$ and $\mathcal{U}_i$ are compact and contain the origin in their interior. The function g_{ij} describes the mutual influences between subsystems. $w_i(k) \in \mathcal{W}_i = \{w_i \in \mathbb{R}^{n_i} : \|w_i\|_{P_i} \leq \xi_i, \xi_i > 0\}$ is the disturbance, and P_i is the positive definite matrix. The set $\mathcal{N}_i^u$ represents the upstream neighbors of subsystem i, i.e., the components of subsystem j's state appear in the dynamics of subsystem i for some $j \in \mathcal{M} \setminus \{i\}$. $\mathcal{N}_i^d$ denotes the downstream neighbors of subsystem i. Note that $j \in \mathcal{N}_i^u$ if and only if $i \in \mathcal{N}_j^d$, for all $i, j \in \mathcal{M}$.

The dynamics of the overall system is

$$\begin{aligned}\dot{x}(t) &= F(x(t), u(t)) + w(t)\\ &= f(x(t), u(t)) + g(x(t)) + w(t),\end{aligned} \tag{3}$$

where $x = [x_1^T, \ldots, x_M^T]^T \in \mathbf{X} \subseteq \mathbb{R}^n$, $\mathbf{X} = \mathcal{X}_1 \times \cdots \times \mathcal{X}_M$, and $u = [u_1^T, \ldots, u_M^T]^T \in \mathbf{U} \subseteq \mathbb{R}^m$, $\mathbf{U} = \mathcal{U}_1 \times \cdots \times \mathcal{U}_M$, $w = [w_1^T, \ldots, w_M^T]^T \in \mathbf{W} \subseteq \mathbb{R}^n$, $\mathbf{W} = \mathcal{W}_1 \times \cdots \times \mathcal{W}_M$, and $n = \sum_{i\in\mathcal{M}} n_i$, $m = \sum_{i\in\mathcal{M}} m_i$. Furthermore, $f(x, u) = [f_1(x_1, u_1)^T, \ldots, f_M(x_M, u_M)^T]^T$ and $g(x) = [\sum_{j\in\mathcal{N}_1^u} g_{1j}(x_j)^T, \ldots, \sum_{j\in\mathcal{N}_M^u} g_{Mj}(x_j)^T]^T$.

Assumption 1 (*Dunbar, 2007*)**.** The function f_i and g_{ij} are twice continuous differentiable and satisfy $f_i(0, 0) = 0$, $g_{ij}(0) = 0$. Furthermore, the system (1) has a unique, absolutely continuous solution for any initial condition $x_i(0)$, any piecewise right-continuous $x_j : [0, \infty) \to \mathcal{X}_j, j \in \mathcal{N}_i^u$, and any piecewise right-continuous $u_i : [0, \infty) \to \mathcal{U}_i$.

Assumption 2 (*Liu et al., 2020*)**.** The function f_i is Lipschitz continuous in its argument, i.e., there exists a constant L_{f_i} depending on the positive definite matrix P_i such that

$$\|f_i(\upsilon, u) - f_i(\varsigma, u)\|_{P_i} \leq L_{f_i}\|\upsilon - \varsigma\|_{P_i} \tag{4}$$

for all $(\upsilon, \varsigma, u) \in \mathcal{X}_i \times \mathcal{X}_i \times \mathcal{U}_i$.

The main objective of this paper is to design a self-triggered DMPC strategy to stabilize the overall system in (3). This strategy has two advantages: (i) the proposed strategy is simple in design and can achieve good control performance; (ii) the triggering frequency can be significantly reduced to save communication resources.

2.2. Preliminaries

This section gives some preliminaries, which will be used in the following design and analysis.

First, we introduce some dynamics to facilitate the design of the terminal set and local state feedback law, which will be used in feasibility and stability analysis. Based on (1), the nominal decoupled dynamics of (1) is expressed as

$$\dot{x}_i(t) = f_i(x_i(t), u_i(t)). \tag{5}$$

Similarly, the nominal dynamics of (3) is

$$\dot{x}(t) = F(x(t), u(t)). \tag{6}$$

Consider the linearized system of (1) and (3) around the origin. The linearization of (1) around the origin is denoted as

$$\dot{x}_i(t) = A_{ii}x_i(t) + B_iu_i(t) + \sum_{j\in\mathcal{N}_i^u} A_{ij}x_j(t) + w_i(t), \tag{7}$$

where $A_{ii} = \partial f_i/\partial x_i(0, 0)$, $A_{ij} = \partial g_{ij}/\partial x_j(0)$ for $j \in \mathcal{N}_i^u$, and $B_i = \partial f_i/\partial u_i(0, 0)$.

The linearization of (3) around the origin is denoted as

$$\dot{x}(t) = Ax(t) + Bu(t) + w(t), \tag{8}$$

where $A = \partial F/\partial x(0, 0)$, $B = \partial f/\partial u(0, 0)$.

Based on the above dynamics, the following two lemmas are given. Lemma 1 shows that there exists a positive invariant set for nominal dynamics in (5) with the local state feedback law. Before giving Lemma 1, an assumption is given.

Assumption 3. For each subsystem i,($i \in \mathcal{M}$), there exists a decoupled state feedback law K_i such that $A_{si} = A_{ii} + B_iK_i$ and $A_o = A + BK$ are both Hurwitz, where $K = \mathrm{Diag}(K_1, \ldots, K_M)$.

Lemma 1 (*Li, Yan, Shi, & Wang, 2015*)**.** *For the nominal decoupled subsystem in (5) with Assumption 3 and any given symmetric matrices $Q_i > 0, R_i > 0$, there exist a constant $\epsilon_i > 0$, a matrix P_i, and a state feedback law $u_i(t) = K_ix_i(t) \in \mathcal{U}_i$ such that: (i) The set $\phi_i(\epsilon_i) = \{x_i(t) \in \mathbb{R}^{n_i} : V_{f_i}(x_i(t)) \leq \epsilon_i^2\}$ is a positive invariant set for subsystem in (5) with $u_i(t) = K_ix_i(t) \in \mathcal{U}_i$; (ii) $\dot{V}_{f_i}(x(t))|_{\dot{x}_i(t)=f_i(x_i(t),K_ix_i(t))} \leq -\|x(t)\|_{\bar{Q}_i}^2$, $\forall x(t) \in \phi_i(\epsilon_i)$. Here, $V_{f_i}(x(t)) = \|x(t)\|_{P_i}^2$, $\bar{Q}_i = Q_i + K_i^TR_iK_i$, and P_i is the solution of the Lyapunov function $P_iA_{si} + A_{si}^TP_i = -\bar{Q}_i$.*

Denote $Q = \mathrm{Diag}\{Q_1, \ldots, Q_M\}$, $P = \mathrm{Diag}\{P_1, \ldots, P_M\}$, $\bar{Q} = \mathrm{Diag}\{\bar{Q}_1, \ldots, \bar{Q}_M\}$, and $A_s = \mathrm{Diag}\{A_{s1}, \ldots, A_{sM}\}$, where Q_i, P_i, $\bar{Q}_i$ and A_{si} are defined in Lemma 1 and Assumption 3, respectively.

Assumption 4 (*Dunbar, 2007*)**.** The inequality $A_o^TP + PA_o - (A_s^TP + PA_s) \leq 1/2\bar{Q}$ holds.

Based on Assumption 4, the positive invariant set $\phi(\varepsilon)$ for nominal system (6) with the state feedback law K can be established, which is elaborated in the following Lemma 2.

Lemma 2. *For the overall system in (3) with Assumption 1, 3 and 4, there exist a constant $\varepsilon > 0$ and a state feedback law $u(x) = Kx(t) \in \mathcal{U}$ such that the set $\phi(\varepsilon) = \{x(t) \in \mathbb{R}^n : V_f(x(t)) \leq \varepsilon^2\}$ is a positive invariant set for system $\dot{x}(t) = F(x(t), Kx(t))$.*

Proof. The proof follows the same line of Dunbar (2007) and Liu et al. (2020), we give a concise proof here.

According to Assumption 4, the derivation of $V_f(x(t))$ can be computed as follows

$$\begin{aligned}&\dot{V}_f(x(t))|_{\dot{x}(t)=F(x(t),Kx(t))}\\ =&x(t)^T(A_o^TP + PA_o)x(t) + 2x(t)^TP\psi(x(t))\\ \leq& -\|x(t)\|_{\bar{Q}}^2\Big(\frac{1}{2} - \frac{2\|\psi(x(t))\|_P}{\lambda_{\min}(P^{-1/2}\bar{Q}P^{-1/2})\|x(t)\|_P}\Big),\end{aligned} \tag{9}$$

where $\psi(x(t)) = F(x(t), Kx(t)) - A_ox(t)$. Since $\frac{\|\psi(x(t))\|_P}{\|x(t)\|_P} \to 0$ as $\|x(t)\|_P \to 0$. There exist constant ε, and $0 < \beta < 1/2$ such that $\frac{\|\psi(x(t))\|_P}{\|x(t)\|_P} \leq (1-2\beta)\lambda_{\min}(P^{-1/2}\bar{Q}P^{-1/2})/4$ such that $\dot{V}_f(x(t)) \leq -\beta\|x(t)\|_{\bar{Q}}^2$ holds for all $x(t) \in \phi(\varepsilon)$. This completes the proof.

3. Rolling self-triggered DMPC

3.1. Dual-model OCP

Under the self-triggered strategy, information sampling and control updating occur asynchronously between different subsystems. For each subsystem i, denote $t_i^r, r \in \mathbb{N}$ as its rth triggering instant. To obtain an accurate prediction of the state evolution of subsystem i, an ideal way is to exploit the actual state information of its upstream neighbors $j \in \mathcal{N}_i^u$. However, the actual state information of its upstream neighbors is not available for subsystem i due to the asynchronous triggering manner. Therefore, at each

triggering instant t_i^r, each subsystem i constructs the assumed state information based on the latest information received from its neighbors, denoted by $x_j^a, j \in \mathcal{N}_i^u$. Similarly, subsystem i transmits its predictive state x_i^a to its downstream neighbors $j, j \in \mathcal{N}_i^d$.

To facilitate the OCP definition, we summarize the notation of different types of state and control input trajectories. For ease of representation, let $\cdot(t; t_i^r)$ be a variable at time t, where $t \in [t_i^r, t_i^r + T]$.

- $\tilde{u}_i(t; t_i^r)$ and $\tilde{x}_i(t; t_i^r)$ are the predicted control input and state trajectory of subsystem i.
- $\tilde{u}_i^*(t; t_i^r)$ and $\tilde{x}_i^*(t; t_i^r)$ are the optimal control input and state trajectory of subsystem i obtained by solving the following OCP.
- $\bar{u}_i(t; t_i^r)$ is a feasible control trajectory candidate and will be constructed in the following part. $\bar{x}_i(t; t_i^r)$ is the feasible state with respect to $\bar{u}_i(t; t_i^r)$.
- $\hat{x}_i(t; t_i^r)$ is the nominal state.
- $x_i^a(t; t_i^r)$ is the assumed state of subsystem i and will be constructed in the following part.

Inspired by Aswani, Gonzalez, Sastry, and Tomlin (2013), the local OCP subsystem i with dual-model is defined by

$$\tilde{u}_i^*(t; t_i^r) = \arg\min \tilde{J}_i(\tilde{x}_i(t; t_i^r), \tilde{u}_i(t; t_i^r))$$

$$\text{s.t. } \dot{\tilde{x}}_i(t; t_i^r) = f_i(\tilde{x}_i(t; t_i^r), \tilde{u}_i(t; t_i^r)) + \sum_{j \in \mathcal{N}_i^u} g_{ij}(x_j^a(t; t_i^r)) \tag{10a}$$

$$\dot{\hat{x}}_i(t; t_i^r) = f_i(\hat{x}_i(t; t_i^r), \tilde{u}_i(t; t_i^r)) \tag{10b}$$

$$\hat{x}_i(t_i^r; t_i^r) = \tilde{x}_i(t_i^r; t_i^r) = x(t_i^r) \tag{10c}$$

$$\hat{x}_i(t; t_i^r) \in \mathcal{X}_i \ominus \mathcal{B}_i(t - t_i^r) \tag{10d}$$

$$\hat{x}_i(t_i^r + T; t_i^r) \in \phi_i(\alpha_i \varepsilon_i) \tag{10e}$$

$$\tilde{u}_i(t; t_i^r) \in \mathcal{U}_i \tag{10f}$$

$$H_i(\hat{x}_i(t; t_i^r), \tilde{u}_i(t; t_i^r)) \le H_i(\bar{x}_i(t; t_i^r), \bar{u}_i(t; t_i^r)) \tag{10g}$$

where $t \in [t_i^r, t_i^r + T]$, T is the prediction horizon. The tightened set $\mathcal{B}_i(t - t_i^r)$, which is designed to satisfy the actual state constraint, will be defined latter. $\phi_i(\alpha_i \varepsilon_i) = \{x \in \mathbb{R}^{n_i} : \|x\|_{P_i} \le \alpha_i \varepsilon_i\}$ denotes the terminal set, where $\varepsilon_i = \min\{\epsilon_i, \varepsilon/\sqrt{M}\}$.

The coupled dynamics in (10a) is employed to guarantee a good control performance. The nominal dynamics in (10b) is used to guarantee the recursive feasibility. The initial state of (10a) and (10b) is regarded in (10c). The tightened constraint in (10d) is designed to satisfy the recursive feasibility and actual state constraint. (10e) is the terminal constraint. The last constraint in (10g) is imposed to ensure the stability of each subsystem.

- The assumed state $x_j^a(t; t_i^r), t \in [t_i^r, t_i^r + T], j \in \mathcal{N}_i^u$ is constructed as

$$x_j^a(t; t_i^r) = \begin{cases} \tilde{x}_j^*(t; \eta_j(t_i^r)), t \in [t_i^r, \eta_j(t_i^r) + T] \\ A_{sj} x_j^a(t; t_i^r), t \in [\eta_j(t_i^r) + T, t_i^r + T], \end{cases} \tag{11}$$

  where $\eta_j(t_i^r) \triangleq \max\{l \in \mathbb{N} : t_j^l \le t_i^r\}$.
- The tightened set $\mathcal{B}_i(t - t_i^r)$ is defined as

$$\mathcal{B}_i(t - t_i^r) := \{x \in \mathbb{R}^{n_i} : \|x\|_{P_i} \le \frac{\xi_i + \theta_{ij}}{L_{f_i}} (e^{L_{f_i}(t - t_i^r)} - 1)\}, \tag{12}$$

  where $\theta_{ij} = \sup_{x_j \in \mathcal{X}_j} \|g_{ij}(x_j)\|_{P_i}$.
- The cost function $\tilde{J}_i(\tilde{x}_i(t; t_i^r), \tilde{u}_i(t; t_i^r))$ is allowed to be any convex function, such as a quadratic function

$$\tilde{J}_i(\tilde{x}_i(t; t_i^r), \tilde{u}_i(t; t_i^r)) = \int_{t_i^r}^{t_i^r + T} (\|\tilde{x}_i(s; t_i^r)\|_{\tilde{Q}_i} + \|\tilde{u}_i(s; t_i^r)\|_{\tilde{R}_i}) ds + \|\hat{x}_i(t_i^r + T; t_i^r)\|_{\tilde{P}_i} \tag{13}$$

  with $\tilde{Q}_i \succ 0$, $\tilde{R}_i \succ 0$, and $\tilde{P}_i \succ 0$, or a linear function $\tilde{J}_i(\tilde{x}_i(t), \tilde{u}_i(t)) = \int_0^T \alpha x_i(s) + \beta \tilde{u}_i(s) ds$ with the weighting vectors α and β. In practice, the choice of $\tilde{J}_i$ is based on practical performance requirements.
- The function $H_i(\hat{x}_i(t; t_i^r), \tilde{u}_i(t; t_i^r))$ is defined as

$$H_i(\hat{x}_i(t; t_i^r), \tilde{u}_i(t; t_i^r)) = \int_{t_i^r}^{t_i^r + T} (\|\hat{x}_i(s; t_i^r)\|_{Q_i}^2 + \|\tilde{u}_i(s; t_i^r)\|_{R_i}^2) ds + \|\hat{x}_i(t_i^r + T; t_i^r)\|_{P_i}^2, \tag{14}$$

  where $Q_i \succ 0$, $R_i \succ 0$, and $P_i \succ 0$. In addition, P_i is the solution of the Lyapunov equation $A_{si}^T P_i + P_i A_{si} = -Q_i$.
- The feasible control input candidate $\bar{u}_i(t; t_i^r), r > 0$ is constructed as

$$\bar{u}_i(t; t_i^r) = \begin{cases} \tilde{u}^*(t; t_i^{r-1}), & t \in [t_i^r, t_i^{r-1} + T], \\ K_i \bar{x}(t; t_i^r), & t \in [t_i^{r-1} + T, t_i^r + T], \end{cases} \tag{15}$$

  where the feasible state trajectory is subject to nominal system dynamics (5) with $\bar{x}_i(t; t_i^r) = x_i(t_i^r)$.

Remark 1. The designed dual-model OCP in (10) is distinct from the conventional ones in the following three noteworthy aspects.

(a) Compared with the conventional OCPs in Alessio et al. (2011), Jia and Krogh (2002), Liu et al. (2014), Ma, Liu, Zhang, and Xia (2020), Magni and Scattolini (2006) and Shalmani et al. (2020) that only employ a single predictive model (the nominal dynamics in (10b) or the coupled dynamics in (10a)), the most significant difference is that the two predictive models are both considered. Such a dual-model OCP enables us to separate the performance guarantee and constraint satisfaction. That is, the performance is guaranteed by finding the control inputs such that the cost function $\tilde{J}_i$ subject to the coupled dynamics (10a) is minimized, and the constraints subject to the nominal dynamics (10b) are checked under the same control inputs. In this way, the control parameters design is simple and the control performance is relatively good.

(b) Compared with previous works on coupled systems, such as Dunbar (2007), Liu et al. (2020) and Zhou et al. (2022), some constraints, in which some parameters require to be designed to satisfy some stringent conditions, are avoided in the OCP (10). One may note that a stability constraint is introduced, however, it can be trivially satisfied without any extra conditions, which is shown in Section 4.2. In this way, the DMPC algorithm is much simpler in design.

(c) The stability constraint (10g) in the OCP is added to reduce the conservativeness in stability analysis. Indeed, the optimal cost subject to the coupled dynamics serves as a Lyapunov function in many works (Dunbar, 2007; Mirzaei & Ramezani, 2021). However, due to the coupling influences in the predicted model, the analysis of the difference in the optimal cost $\tilde{J}_i$ between two successive updates is quite conservative, leading to conservative sufficient conditions for ensuring stability. Therefore, we construct the

function H_i as the Lyapunov function candidate and impose the stability constraint (10g) on it to solve the above challenge.

Remark 2.

(a) The stability and performance can be decoupled by the dual-model strategy. As a result, stability no longer depends on the cost function $\tilde{J}_i$. Therefore, any arbitrary quadratic function is allowed. In practice, the choice of $\tilde{J}_i$ is based on practical performance requirements. For example, in simplified adaptive cruise control (Lin, Görges, & Weißmann, 2017), it is chosen as $\tilde{J}_i = \int_0^T a_i(s)^2 ds$ for driving comfort and energy efficiency where $a_i = u_i$ is the acceleration, and in the control of room temperature in summer scenario (Dai, Qiang, Sun, Zhou, & Xia, 2020), it is chosen as $\tilde{J}_i = \int_0^T \alpha|\tilde{x}_i(s) - x_{i,d}| + \beta|\tilde{u}_i(s)|ds$ for the degree of comfort to the indoor temperature and the cost of power.

(b) The function H_i is proposed to ensure the stability, the choice of which is restricted. Once the weighting matrices Q_i, R_i are given, $\bar{Q}_i = Q_i + K_i R_i K_i$ is determined, and then P_i can be obtained by solving the Lyapunov equation $(A_{ii} + B_i K_i)^T P_i + P_i(A_{ii} + B_i K_i) = -\bar{Q}_i$.

3.2. Rolling self-triggered mechanism

The actual state trajectory (1) and the nominal one (5) of subsystem i are both generated by employing control input $\tilde{u}_i^*(t; t_i^r)$. However, the ignorance of coupling terms and external disturbance in dynamics (5) causes state error between $x(t)$ and $\hat{x}_i(t; t_i^r)$. The following lemma formulates this deviation, which is a prerequisite for the design of the self-triggering mechanism.

Lemma 3. *For each subsystem i, if the actual system (1) and the nominal one (5) are both controlled by the control input $\tilde{u}_i^*(t; t_i^r)$, then actual state predictive error $\|x_i(t) - \hat{x}_i(t; t_i^r)\|_{P_i}$ is bounded by*

$$\|x_i(t) - \hat{x}_i(t; t_i^r)\|_{P_i} \le \frac{\xi_i + \theta_{ij}}{L_{f_i}}(e^{L_{f_i}(t-t_i^r)} - 1), \tag{16}$$

where $t \in [t_i^r, t_i^r + T]$.

Proof. The proof can be easily completed by using Gronwall–Bellman inequality, and thus omitted.

Considering the recursive feasibility of the OCP, it is required that the actual state trajectory does not deviate far away from the nominal state trajectory. To that end, conventional self-triggered mechanisms, such as Eqtami et al. (2013), Hashimoto et al. (2014) and Sun et al. (2019), use the estimated state predictive error and a triggering threshold to design the triggering condition as follows

$$\begin{aligned}\frac{\xi_i + \theta_{ij}}{L_{f_i}}(e^{L_{f_i}(t-t_i^r)} - 1) &= (\varepsilon_i - \alpha_i\varepsilon_i)e^{L_{f_i}(t-t_i^r-T)} \\ &=: \varphi(t),\end{aligned} \tag{17}$$

where $\varphi(t)$ is a time-varying triggering threshold that is designed to guarantee the recursive feasibility. The design of $\varphi(t)$ can be seen in Section 4.2.

Solving (17) yields the triggering instants as follows

$$t_i^{r+1} := \inf\{t : t > t_i^r, (17)\}. \tag{18}$$

Using the upper bounds of coupling terms and disturbances to evaluate actual state predictive error leads to a conservative result since the actual coupling terms and disturbances cannot be obtained. As a result, the triggering determined by (18) is frequent.

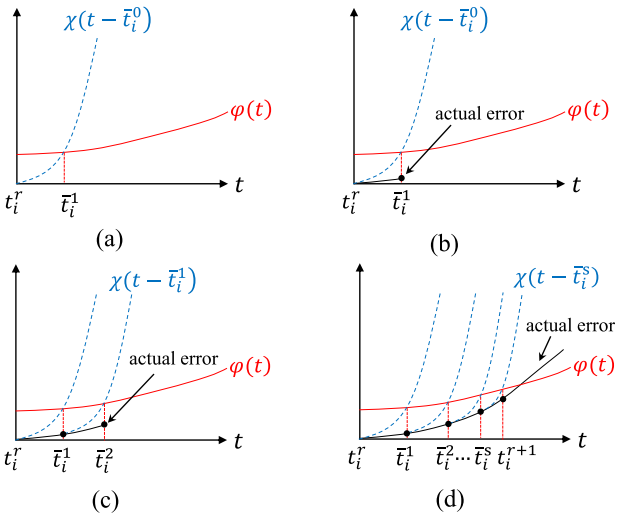

Fig. 1. Rolling self-triggered mechanism. (a) At triggering instant t_i^r, the 1st sampling instant $\bar{t}_i^1$ is determined by (21). (b) At $\bar{t}_i^1$, the current state $x_i(\bar{t}_i^1)$ is measured and the actual value of $\|x_i(\bar{t}_i^1) - \hat{x}_i(\bar{t}_i^1; t_i^r)\|_{P_i}$ is obtained. (c) $\chi(t - \bar{t}_i^1)$ is calculated by (19), and the next sampling instant $\bar{t}_i^2$ is determined by (21). (d) The process in (b) and (c) is performed repeatedly until the stop condition in (22) is satisfied, and the next triggering instant t_i^{r+1} is determined by (23).

To overcome this drawback, we add some sampling of the states in a rolling manner to obtain a less conservative evaluation of the actual state predictive error. To be specific, we first define $\bar{t}_i^s$ as the sth sampling instant after t_i^r, i.e., $\bar{t}_i^s \ge t_i^r$, $\bar{t}_i^0 = t_i^r$, $s \in \mathbb{Z}$. At each sampling instant $\bar{t}_i^s$, the current state $x_i(\bar{t}_i^s)$ is measured and the actual value of $\|x_i(\bar{t}_i^s) - \hat{x}_i(\bar{t}_i^s; t_i^r)\|_{P_i}$ is calculated. Based on this actual value, a more accurate evaluation of $\|x_i(t) - \hat{x}_i(t; t_i^r)\|_{P_i}$, $t > \bar{t}_i^s$ can be obtained, and based on which, the next sampling instant $\bar{t}_i^{s+1}$ is then determined by the conventional self-triggered mechanism. The whole process is illustrated in Fig. 1.

In the following three parts, we explicitly formulate the proposed rolling self-triggered mechanism.

Firstly, we evaluate $\|x_i(t) - \hat{x}_i(t; t_i^r)\|_{P_i}$, $t > \bar{t}_i^s$ by using the actual value of $\|x_i(\bar{t}_i^s) - \hat{x}_i(\bar{t}_i^s; t_i^r)\|_{P_i}$ in Lemma 4.

Lemma 4. *For each subsystem i, the predictive error between $x(t)$ and $\hat{x}_i(t; t_i^r)$ is bounded by*

$$\begin{aligned}\|x_i(t) - \hat{x}_i(t; t_i^r)\|_{P_i} &\le \|x_i(\bar{t}_i^s) - \hat{x}_i(\bar{t}_i^s; t_i^r)\|_{P_i} e^{L_{f_i}(t-\bar{t}_i^s)} \\ &\quad + \frac{\xi_i + \theta_{ij}}{L_{f_i}}(e^{L_{f_i}(t-\bar{t}_i^s)} - 1) \\ &:= \chi(t - \bar{t}_i^s),\end{aligned} \tag{19}$$

where $t \in [t_i^r, t_i^r + T]$, $\bar{t}_i^s \in [t_i^r, t]$, and $\chi(t - \bar{t}_i^s)$ represents the evaluation of the actual state predictive error.

Proof. According the actual system dynamics (1) and the nominal one (5), we obtain

$$\begin{aligned}&\|x_i(t) - \hat{x}_i(t; t_i^r)\|_{P_i} \\ =&\|x_i(\bar{t}_i^s) + \int_{\bar{t}_i^s}^{s}(f_i(x_i(s), \tilde{u}_i^*(s; t_i^r)) + \sum_{j\in\mathcal{N}_i^u} g_{ij}(x_j(s)) \\ &+ w_i(s))ds - \hat{x}_i(\bar{t}_i^s; t_i^r) - \int_{\bar{t}_i^s}^{s} f_i(\hat{x}_i(s; t_i^r), \tilde{u}_i^*(s; t_i^r))ds\|_{P_i} \\ \le&\|x_i(\bar{t}_i^s) - \hat{x}_i(\bar{t}_i^s; t_i^r)\|_{P_i} + (\theta_{ij} + \xi_i)(t - \bar{t}_i^s)\end{aligned}$$

$$+\int_{\bar{t}_i^s}^{s} L_{f_i}\|x_i(s)-\hat{x}_i(s;t_i^r)\|ds$$

$$\leq \|x_i(\bar{t}_i^s)-\hat{x}_i(\bar{t}_i^s;t_i^r)\|_{P_i}e^{L_{f_i}(t-\bar{t}_i^s)}+\frac{\xi_i+\theta_{ij}}{L_{f_i}}(e^{L_{f_i}(t-\bar{t}_i^s)}-1),$$

where the last inequality uses the Gronwall–Bellman inequality.

Secondly, we determine the sampling instant $\bar{t}_i^s$ by using the conventional self-triggered mechanism. Specifically, the update condition is designed as follows

$$\begin{aligned}&\|x_i(\bar{t}_i^s)-\hat{x}_i(\bar{t}_i^s;t_i^r)\|_{P_i}e^{L_{f_i}(t-\bar{t}_i^s)}+\frac{\xi_i+\theta_{ij}}{L_{f_i}}(e^{L_{f_i}(t-\bar{t}_i^s)}-1)\\&=(\varepsilon_i-\alpha_i\varepsilon_i)e^{L_{f_i}(t-t_i^r-T)},\ \ \bar{t}_i^0=t_i^r.\end{aligned}\tag{20}$$

By virtue of (20), the sampling instant $\bar{t}_i^{s+1}, s\in\mathbb{Z}$ is determined by

$$\bar{t}_i^{s+1}:=\inf\{t: t>\bar{t}_i^s,(20)\}.\tag{21}$$

Thirdly, we establish the stop condition of sampling, which also determines the next triggering instant t_i^{r+1}. The main idea is that if two successive sampling instants $\bar{t}_i^s$ and $\bar{t}_i^{s+1}$ are sufficiently close, the state predictive error $\|x_i(\bar{t}_i^s)-\hat{x}_i(\bar{t}_i^s;t_i^r)\|_{P_i}$ may be close to the triggering threshold $\varphi(t)$ in (17). Therefore, we simply set $t_i^{r+1}=\bar{t}_i^s$. Moreover, the constraint $t_i^{r+1}\leq t_i^r+T$ should also be satisfied. In summary, the stop condition is set by

$$\bar{t}_i^{s+1}-\bar{t}_i^s<\delta_i\quad\text{or}\quad\bar{t}_i^{s+1}-t_i^r\geq T,\tag{22}$$

and the next triggering instant is then determined as follows:

$$t_i^{r+1}=\begin{cases}\bar{t}_i^s, & \text{if } \bar{t}_i^{s+1}-\bar{t}_i^s<\delta_i,\\ t_i^r+T, & \text{if } \bar{t}_i^{s+1}-t_i^r\geq T,\end{cases}\tag{23}$$

where δ_i is the minimum sampling interval for each subsystem i.

From triggering instant t_i^r, the sampling process is carried out with the initial condition $\bar{t}_i^0=t_i^r$ until the stop condition in (22) is satisfied. This sampling process enters the next cycle starting from t_i^{r+1}. The sampling instant is determined based on the conventional self-triggered mechanism in a rolling manner, thus the name of "rolling self-triggered mechanism". Obviously, the conventional self-triggering mechanism is a special case of the proposed rolling self-triggered mechanism. Therefore, the propose one can save communication resources more efficiently.

Algorithm 1 Rolling Self-Triggered DMPC Algorithm

1: At time $t=0$, set $r=0$, $s=0$, $\bar{t}_i^s=0$, $x_j^a(t;t_i^r)=0$, flag $=1$, solve the OCP in (10), and determine the next sampling instant $\bar{t}_i^{s+1}$ according to (21), go to step 5.
2: At any time $t>0$, if $x(t)\in\phi(\varepsilon)$, apply control input $Kx(t)$ and go to step 2. Otherwise, go to step 3;
3: If $t=t_i^r$, set flag $=1$, construct the assumed states $x_j^a(t;t_i^r), j\in\mathcal{N}_i^u$ according to (11); solve the OCP in (10) and transmit $\tilde{x}_i^*(t;t_i^r), t\in[t_i^r,t_i^r+T]$ to downstream neighbors $j, j\in\mathcal{N}_i^d$; set initial sampling instant $\bar{t}_i^0=t, s=0$; determine the next sampling instant $\bar{t}_i^{s+1}$ according to (21) and go to step 5. Otherwise, go to step 4;
4: If $t=\bar{t}_i^s$, determine the next sampling instant $\bar{t}_i^{s+1}$ according to (21). Otherwise, go to step 6.
5: Check the stop condition (22). If it is satisfied, determine the next triggering instant t_i^{r+1} according to (23), and set $r=r+1$, flag $=0$. Otherwise, set $s=s+1$;
6: If flag $=1$, apply the control input $\tilde{u}_i^*(t;t_i^r)$, and go to step 2. Otherwise, apply $\tilde{u}_i^*(t;t_i^{r-1})$, and go to step 2.

4. Analysis

In this section, the theoretical results are given by the following three theorems. Firstly, Theorem 1 states that the Zeno behavior is avoided by the designed Algorithm 1. Secondly, the recursive feasibility is analyzed in Theorem 2, followed by stability analysis in the third one.

4.1. Avoidance of Zeno behavior

Theorem 1 states that there always exists a lower bound of the triggering interval, which means the designed algorithm is Zeno-free.

Theorem 1. *For the system (1) with Algorithm 1. If*

$$\frac{1}{L_{f_i}}\ln\frac{(1-\alpha_i)\varepsilon_i L_{f_i}}{\xi_i+\theta_{ij}}<T\tag{24}$$

is satisfied, then the minimum triggering interval Δ_i, i.e., $\Delta_i\leq\inf_{r\in\mathbb{N}}\{t_i^{r+1}-t_i^r\}$, is

$$\Delta_i=\frac{1}{L_{f_i}}\ln\frac{e^{L_{f_i}T}}{e^{L_{f_i}T}-\frac{(1-\alpha_i)\varepsilon_i L_{f_i}}{\xi_i+\theta_{ij}}}.\tag{25}$$

Proof. Observed from (23), one can easily obtain that $t_i^{r+1}\geq\bar{t}_i^1$. Substituting $\bar{t}_i^s=\bar{t}_i^0$ into (20) yields

$$\frac{\xi_i+\theta_{ij}}{L_{f_i}}(e^{L_{f_i}(t-\bar{t}_i^0)}-1)=(\varepsilon_i-\alpha_i\varepsilon_i)e^{L_{f_i}(t-t_i^r-T)}.$$

Solving the above equation and considering $\bar{t}_i^0=t_i^r$, we can further obtain $\bar{t}_i^1-t_i^r=\Delta_i$. Therefore, $t_i^{r+1}-t_i^r\geq\bar{t}_i^1-t_i^r$, i.e., $\inf_{r\in\mathbb{N}}\{t_i^{r+1}-t_i^r\}\geq\Delta_i$ holds. This completes the proof.

4.2. Recursive feasibility analysis

The recursive feasibility guarantees that the solution of the local OCP always exists for each subsystem i, ($i\in\mathcal{M}$) at each triggering instant provided that an initial feasible solution at $t_i^0=0$ is available. In the following, we first give an initial feasible assumption of the local OCP.

Assumption 5 (*Ma, Liu, Zhang, & Xia, 2020*)**.** The local OCP of each subsystem i, ($i\in\mathcal{M}$) is feasible at initial time and $\phi_i(\varepsilon_i)\subset\mathcal{X}_i\ominus\mathcal{B}_i(T)$.

Theorem 2. *For system (1) with Assumptions 1–5. If the prediction horizon is chosen as*

$$T\leq\frac{1}{L_{f_i}}\ln\frac{(1-\alpha_i)\varepsilon_i L_{f_i}}{(\xi_i+\theta_{ij})(1-\alpha_i 4^{\frac{\lambda_{\max}(P_i)}{\lambda_{\min}(Q_i)}}L_{f_i})},\tag{26}$$

then OCP in (10) is recursively feasible.

Proof. This proof is conducted by induction principle. Firstly, OCP is feasible at $t_i^0=0$. Secondly, suppose that OCP is feasible at $t_i^{r-1}, r>1, i\in\mathcal{M}$. Then, we need to prove that the OCP is also feasible at t_i^r. To prove this, we require to show that the control input candidate $\bar{u}_i(t;t_i^r)$ in (15) and the corresponding state $\bar{x}_i(t;t_i^r)$ satisfy constraints (10d)–(10g).

(1) The satisfaction of the tightened constraint (10d), i.e., $\bar{x}_i(t;t_i^r)\in\mathcal{X}_i\ominus\mathcal{B}_i(t-t_i^r), t\in[t_i^r,t_i^r+T]$: When $t\in[t_i^{r-1},t_i^{r-1}+T]$, based on the constructed control input $\bar{u}_i(t;t_i^r)$, we obtain

$$\begin{aligned}&\|\bar{x}_i(t;t_i^r)-\hat{x}_i(t;t_i^{r-1})\|_{P_i}\\&=\|\bar{x}_i(t_i^r;t_i^r)+\int_{t_i^r}^{s}f_i(\bar{x}_i(s;t_i^r),\tilde{u}_i^*(s;t_i^{r-1}))ds\end{aligned}$$

$$
\begin{aligned}
&- \hat{x}_i(t_i^r; t_i^{r-1}) - \int_{t_i^r}^{s} f_i(\hat{x}_i(s; t_i^{r-1}), \tilde{u}_i^*(s; t_i^{r-1}))ds\|_{P_i} \\
\leq &\|x_i(t_i^r) - \hat{x}_i(t_i^r; t_i^{r-1})\|_{P_i} \\
&+ \int_{t_i^r}^{s} L_{f_i}\|\bar{x}_i(s; t_i^r) - \hat{x}_i(s; t_i^{r-1})\|_{P_i} ds
\end{aligned}
$$

Applying the Gronwall–Bellman inequality yields

$$
\begin{aligned}
&\|\bar{x}_i(t; t_i^r) - \hat{x}_i(t; t_i^{r-1})\|_{P_i} \\
&\leq \|x_i(t_i^r) - \hat{x}_i(t_i^r; t_i^{r-1})\|_{P_i} e^{L_{f_i}(t-t_i^r)}.
\end{aligned} \tag{27}
$$

By virtue of (16), it follows that $\|x_i(t_i^r) - \hat{x}_i(t_i^r; t_i^{r-1})\|_{P_i} \leq \chi(t_i^r - t_i^{r-1}) = \frac{\xi_i+\theta_{ij}}{L_{f_i}}(e^{L_{f_i}(t_i^r - t_i^{r-1})} - 1)$, and then

$$
\begin{aligned}
&\|\bar{x}_i(t; t_i^r) - \hat{x}_i(t; t_i^{r-1})\|_{P_i} \\
&\leq \frac{\xi_i + \theta_{ij}}{L_{f_i}}(e^{L_{f_i}(t-t_i^{r-1})} - e^{L_{f_i}(t-t_i^r)}).
\end{aligned}
$$

Since $\hat{x}_i(t; t_i^{r-1}) \in \mathcal{X}_i \ominus \mathcal{B}_i(t - t_i^{r-1})$, we have $\bar{x}_i(t; t_i^r) \in \mathcal{X}_i \ominus \mathcal{B}_i(t - t_i^{r-1}) \oplus \frac{\xi_i+\theta_{ij}}{L_{f_i}}(e^{L_{f_i}(t-t_i^{r-1})} - e^{L_{f_i}(t-t_i^r)}) \subset \mathcal{X}_i \ominus \mathcal{B}_i(t - t_i^r)$.

When $t \in [t_i^{r-1}+T, t_i^r+T]$, we will show that $\bar{x}_i(t; t_i^r) \in \phi_i(\varepsilon_i)$, which implies that $\bar{x}_i(t; t_i^r) \in \mathcal{X}_i \ominus \mathcal{B}_i(t-t_i^r)$ holds by Assumption 5. In view of (16), (20) and (23), it follows that

$$
\begin{aligned}
&\|x_i(t_i^r) - \hat{x}_i(t_i^r; t_i^{r-1})\|_{P_i} \\
\leq &\|x_i(\bar{t}_i^s) - \hat{x}_i(\bar{t}_i^s; t_i^{r-1})\|_{P_i} e^{L_{f_i}(t_i^r - \bar{t}_i^s)} \\
&+ \frac{\xi_i + \theta_{ij}}{L_{f_i}}(e^{L_{f_i}(t_i^r - \bar{t}_i^s)} - 1) \\
= &(\varepsilon_i - \alpha_i\varepsilon_i)e^{L_{f_i}(t_i^r - t_i^{r-1} - T)},
\end{aligned} \tag{28}
$$

where $\bar{t}_i^s$ is the latest sampling instant before t_i^r.

Substituting (28) into (27), we can also obtain

$$
\|\bar{x}_i(t; t_i^r) - \hat{x}_i(t; t_i^{r-1})\|_{P_i} \leq (\varepsilon_i - \alpha_i\varepsilon_i)e^{L_{f_i}(t - t_i^{r-1} - T)} \tag{29}
$$

Therefore, by setting $t = t_i^{r-1} + T$, it follows $\|\bar{x}_i(t_i^{r-1} + T; t_i^r) - \hat{x}_i(t_i^{r-1} + T; t_i^{r-1})\|_{P_i} \leq (\varepsilon_i - \alpha_i\varepsilon_i)$. Using the triangle inequality yields $\|\bar{x}_i(t_i^{r-1} + T; t_i^r)\|_{P_i} \leq \varepsilon_i$, that is, $\bar{x}_i(t_i^{r-1} + T; t_i^r) \in \phi_i(\varepsilon_i)$, which allows the state feedback control $K_i x_i$ to be used. According to Lemma 1, $\bar{x}_i(t; t_i^r)$, $t \in [t_i^{r-1} + T, t_i^r + T]$ will remain in $\phi_i(\varepsilon_i)$.

(2) The satisfaction of the terminal constraint (10e), i.e., $\bar{x}_i(t_i^r + T; t_i^r) \in \phi_i(\alpha_i\varepsilon_i)$: Since $\bar{x}_i(t_i^{r-1} + T; t_i^r) \in \phi_i(\varepsilon_i)$, Lemma 1 is valid, one has $\dot{V}_{f_i}(\|\bar{x}_i(t; t_i^r)\|_{P_i}) \leq -\|\bar{x}_i(t; t_i^r)\|^2_{\bar{Q}_i}$ for $t \in [t_i^{r-1} + T, t_i^r + T]$. Applying the comparison principle, we further obtain that $\|\bar{x}_i(t; t_i^r)\|^2_{P_i} \leq \|\bar{x}_i(t_i^{r-1} + T; t_i^r)\|^2_{P_i} e^{-\frac{\lambda_{\min}(\bar{Q}_i)}{2\lambda_{\max}(P_i)}(t - t_i^{r-1} - T)}$. Therefore, setting $t = t_i^r + T$ yields $\|\bar{x}_i(t_i^r + T; t_i^r)\|^2_{P_i} \leq \varepsilon_i^2 e^{-\frac{\lambda_{\min}(\bar{Q}_i)}{2\lambda_{\max}(P_i)}(t_i^r - t_i^{r-1})}$. By using $t_i^r - t_i^{r-1} \geq \Delta_i$, (25) and (26), we finally obtain $\|\bar{x}_i(t_i^r + T; t_i^r)\|^2_{P_i} \leq \alpha_i^2\varepsilon_i^2$.

(3) The satisfaction of the control constraint (10f), i.e., $\bar{u}_i(t; t_i^r) \in \mathcal{U}_i$, $t \in [t_i^r, t_i^r + T]$: From the construction of $\bar{u}_i(t; t_i^r)$ in (15), one obtains $\bar{u}_i(t; t_i^r) = \tilde{u}^*(t; t_i^{r-1}) \in \mathcal{U}_i$, $t \in [t_i^{r-1}, t_i^{r-1} + T]$. In view of $\bar{x}_i(t_i^{r-1} + T; t_i^r) \in \phi_i(\varepsilon_i)$ and Lemma 1, $\bar{u}_i(t; t_i^r) = K_i\tilde{x}(t; t_i^r) \in \mathcal{U}_i$, $t \in [t_i^{r-1} + T, t_i^r + T]$.

(4) The satisfaction of the stability constraint (10g), i.e., $H_i(\bar{x}_i(t; t_i^r), \bar{u}_i(t; t_i^r)) \leq H_i(\bar{x}_i(t; t_i^r), \bar{u}_i(t; t_i^r))$: This holds naturally. This completes the proof.

From the above analysis, we can see that the recursive feasibility can be guaranteed if only one sufficient condition (26) is needed. Compared with previous work, the proposed dual-model strategy is much simpler in design.

Remark 3. To guarantee the recursive feasibility of the OCP, initial feasibility is needed. To this end, many works assume that there exists an assumed state trajectory $x_j^a(t; 0)$, $j \in \mathcal{N}_i^u$ such that the solution of the OCP exists at the initial time because the feasibility depends on the coupled model, see, e.g., Dunbar (2007), Kang et al. (2022) and Liu et al. (2020). In this regard, the initial assumed state trajectory $x_j^a(t; 0)$, $j \in \mathcal{N}_i^u$ requires to be chosen carefully to ensure that the solution of the OCP exists. However, such a requirement is avoided in the proposed strategy because the feasibility depends on the decoupled model.

Remark 4. According to (24) and (26), the prediction horizon T can be determined once the control parameters α_i and ε_i are selected. In practical implementation, we want a larger T to ensure the feasibility of the OCP. However, it can be observed from (20) that a larger T gives rise to a smaller triggering threshold, which implies that triggering is more frequent. Therefore, we should choose T carefully.

4.3. Stability analysis

This part establishes the sufficient condition for the stability of the overall system.

Theorem 3. *For the overall system* (3) *with Assumptions* 1–5, *if the following two conditions*

$$
\begin{aligned}
&\frac{L_{Q_i}\lambda_{\max}(\sqrt{Q_i})}{L_{f_i}\lambda_{\min}(\sqrt{P_i})}(\varepsilon_i - \alpha_i\varepsilon_i)(1 - e^{L_{f_i}(\Delta_i - T)}) \\
&\qquad + (1 - \alpha_i^2)\varepsilon_i^2 < \frac{\lambda_{\min}(Q_i)}{\lambda_{\max}(P_i)}\Delta_i(\alpha_i\varepsilon_i)^2
\end{aligned} \tag{30}
$$

$$
\xi \leq \frac{\beta\varepsilon\lambda_{\min}(P^{-1/2}\bar{Q}P^{-1/2})}{2} \tag{31}
$$

are satisfied, then the overall system state will converge to the robust positively invariant set $\phi(\varepsilon)$ under Algorithm 1.

Proof. First, we show that for each subsystem i, $x_i(t), x_i(t) \notin \phi_i(\varepsilon_i)$ will enter into $\phi_i(\varepsilon_i)$ in finite time. The Lyapunov function candidate is chosen as

$$
V_i(t_i^r) := H_i(\hat{x}_i(t; t_i^r), \tilde{u}_i^*(t; t_i^r)). \tag{32}
$$

Due to the stability constraint in (10g), we have $V_i(t_i^r) - V_i(t_i^{r-1}) \leq H_i(\bar{x}_i(t; t_i^r), \bar{u}_i(t; t_i^r)) - H_i(\hat{x}_i(t; t_i^{r-1}), \tilde{u}_i^*(t; t_i^{r-1}))$.

According to (14) and (15), one obtains

$$
\begin{aligned}
&H_i(\bar{x}_i(t; t_i^r), \bar{u}_i(t; t_i^r)) - H_i(\hat{x}_i(t; t_i^{r-1}), \tilde{u}_i^*(t; t_i^{r-1})) \\
= &a + b + c,
\end{aligned} \tag{33}
$$

where $a := -\int_{t_i^{r-1}}^{t_i^r}(\|\hat{x}_i(s; t_i^{r-1})\|^2_{Q_i} + \|\tilde{u}_i(s; t_i^{r-1})\|^2_{R_i})ds$, $b := \int_{t_i^r}^{t_i^{r-1}+T}(\|\bar{x}_i(s; t_i^r)\|^2_{Q_i} - \|\hat{x}_i(s; t_i^{r-1})\|^2_{Q_i})ds$, and $c := \int_{t_i^{r-1}+T}^{t_i^r+T}(\|\bar{x}_i(s; t_i^r)\|^2_{Q_i} + \|\bar{u}_i(s; t_i^r)\|^2_{R_i})ds + \|\bar{x}_i(t_i^r + T; t_i^r)\|^2_{P_i} - \|\hat{x}_i(t_i^{r-1} + T; t_i^{r-1})\|^2_{P_i}$. For $s \in [t_i^{r-1}, t_i^r]$, one can obtain $\|x_i(s) - \hat{x}_i(s; t_i^{r-1})\|_{Q_i} \leq (1 - \alpha_i)\varepsilon_i$ according to (28). Since $x_i(t) \notin \phi_i(\varepsilon_i)$, then it follows that $\|\hat{x}_i(s; t_i^{r-1})\|_{Q_i} \geq \|\hat{x}_i(s; t_i^{r-1})\|_{Q_i} - \|x_i(s) - \hat{x}_i(s; t_i^{r-1})\|_{Q_i} \geq \alpha_i\varepsilon_i$. Therefore,

$$
a \leq -\int_{t_i^{r-1}}^{t_i^r}(\|\hat{x}_i(s; t_i^{r-1})\|^2_{Q_i})ds \leq -\frac{\lambda_{\min}(Q_i)}{\lambda_{\max}(P_i)}\Delta_i(\alpha_i\varepsilon_i)^2. \tag{34}
$$

According to Paulavičius and Žilinskas (2006), there always exist constants L_{Q_i} and L_{P_i} such that $\|x\|^2_{Q_i} - \|y\|^2_{Q_i} \leq L_{Q_i}\|x - y\|_{Q_i}$ and $\|x\|^2_{P_i} - \|y\|^2_{P_i} \leq L_{P_i}\|x - y\|_{P_i}$ for all $x, y \in \mathcal{X}_i$, $i \in \mathcal{M}$. Thus, b

can be calculated as

$$
\begin{aligned}
b \leq & \int_{t_i^r}^{t_i^{r-1}+T} L_{Q_i}(\|\bar{x}_i(s;t_i^r)-\hat{x}_i(s;t_i^{r-1})\|_{Q_i})ds \\
\leq^{(29)} & \int_{t_i^r}^{t_i^{r-1}+T} \frac{\lambda_{\max}(Q_i)}{\lambda_{\min}(P_i)} L_{Q_i}(\varepsilon_i-\alpha_i\varepsilon_i)e^{L_{f_i}(s-t_i^{r-1}-T)}ds \\
\leq & \frac{L_{Q_i}\lambda_{\max}(Q_i)}{L_{f_i}\lambda_{\min}(P_i)}(\varepsilon_i-\alpha_i\varepsilon_i)(1-e^{L_{f_i}(\Delta_i-T)}). \qquad (35)
\end{aligned}
$$

Considering Lemma 1, it follows that

$$
\begin{aligned}
c \leq & \|\bar{x}_i(t_i^{r-1}+T;t_i^r)\|_{P_i}^2 - \|\bar{x}_i(t_i^r+T;t_i^r)\|_{P_i}^2 \\
& - \|\bar{x}_i(t_i^r+T;t_i^r)\|_{P_i}^2 - \|\hat{x}_i(t_i^{r-1}+T;t_i^{r-1})\|_{P_i}^2 \\
\leq^{(29)} & (1-\alpha_i^2)\varepsilon_i^2. \qquad (36)
\end{aligned}
$$

Combining (34), (35) and (36), we obtain

$$
\begin{aligned}
& V_i(t_i^r)-V_i(t_i^{r-1}) \\
\leq & -\frac{\lambda_{\min}(Q_i)}{\lambda_{\max}(P_i)}\Delta_i(\alpha_i\varepsilon_i)^2 + L_{P_i}(\varepsilon_i-\alpha_i\varepsilon_i) \\
& + \frac{L_{Q_i}\lambda_{\max}(Q_i)}{L_{f_i}\lambda_{\min}(P_i)}(\varepsilon_i-\alpha_i\varepsilon_i)(1-e^{L_{f_i}(\Delta_i-T)}) \\
<^{(30)} & 0.
\end{aligned}
$$

By using the same argument as the Theorem 1 in Chen and Allgöwer (1998), the state $x(t) \notin \phi(\varepsilon)$ will enter into $\phi(\varepsilon)$ in finite time.

Second, we show that the overall system state will stay in $\phi(\varepsilon)$ forever. From Lemma 2, the derivation of $x(t)^T P x(t)$ along the system trajectory $\dot{x}(t) = F(x(t), u(t)) + w(t)$ yields

$$
\begin{aligned}
& \dot{V}_f(x(t))|_{\dot{x}(t)=F(x(t),Kx(t))+w(t)} \\
\leq & -\|x(t)\|_{\bar{Q}}^2\left(\beta - \frac{2\|w(t)\|_P}{\lambda_{\min}(P^{-1/2}\bar{Q}P^{-1/2})\|x(t)\|_P}\right) \\
\leq^{(31)} & 0,
\end{aligned}
$$

which implies $\phi(\varepsilon)$ is a robust positive invariant set. This completes the proof.

Remark 5. Theorems 2–3 establish the sufficient conditions for guaranteeing the recursive feasibility of the OCP and the stability of the overall systems and also provide guidance on control parameter selection. In practical implementation, one can follow the following steps to determine control parameters.

(i) Choose matrixes Q_i, R_i, and P_i, $i \in \mathcal{M}$ and determine the terminal set $\phi_i(\varepsilon_i)$ according to Lemmas 1 and 2.

(ii) Calculate ξ_i and θ_{ij} based on system dynamics, and then choose an appropriate α_i to determine the predictive horizon T and the minimum triggering interval Δ_i according to (24)–(26) and (30).

5. Simulation example

This section verifies the effectiveness of the proposed self-triggered DMPC strategy by applying it to three similar cart-spring–damper subsystems (Liu et al., 2014).

The dynamics of three subsystems are described as:

$$
\begin{aligned}
\dot{x}_{11}(t) &= x_{12}(t) \\
\dot{x}_{12}(t) &= -\tfrac{k_d}{m}x_{12}(t) - \tfrac{k_s}{m}e^{-x_{11}(t)}x_{11}(t) \\
&\quad - \tfrac{k_c}{m}(x_{11}(t)-x_{21}(t)) + \tfrac{1}{m}u_1 + w_1(t) \\
\dot{x}_{21}(t) &= x_{22}(t) \\
\dot{x}_{22}(t) &= -\tfrac{k_d}{m}x_{22}(t) - \tfrac{k_s}{m}e^{-x_{21}(t)}x_{21}(t) \\
&\quad - \tfrac{k_c}{m}(x_{21}(t)-x_{11}(t)) - \tfrac{k_c}{m}(x_{21}(t) \\
&\quad - x_{31}(t)) + \tfrac{1}{m}u_2 + w_2(t) \\
\dot{x}_{31}(t) &= x_{32}(t) \\
\dot{x}_{32}(t) &= -\tfrac{k_d}{m}x_{32}(t) - \tfrac{k_s}{m}e^{-x_{31}(t)}x_{31}(t) \\
&\quad - \tfrac{k_c}{m}(x_{31}(t)-x_{21}(t)) + \tfrac{1}{m}u_3 + w_3(t)
\end{aligned}
$$

where x_{i1} and x_{i2} are the displacement and the velocity of cart $i(i = 1, 2, 3)$, respectively. m is the mass of each cart; k_d and k_s are the local viscous damping and the stiffness of the local nonlinear spring of each cart, respectively; k_c is the stiffness of the interconnecting spring; u_i is control input; w_i is external disturbance. The numerical values for each cart are selected as: $m = 1.25$ kg, $k_s = 0.7$ N/m, $k_d = 1.3$ Ns/m, $k_c = 0.005$ N/m. The external disturbance $w_i = 0.0027$, $i = 1, 2, 3$. The state and control input constraints are $\mathcal{X}_i = \{x_i : -1\text{ m} \leq x_{i1} \leq 1\text{ m}, -1\text{ m/s} \leq x_{i2} \leq 1\text{ m/s}\}$ and $\mathcal{U}_i = \{u_i : -1\text{N} \leq u_i \leq 1\text{N}\}$. The initial states of the three carts are $x_1(0) = [0.5,\ 0]$, $x_2(0) = [0.5,\ 0]$, and $x_3(0) = [-0.55,\ 0]$.

To conduct Algorithm 1, the sampling interval $\delta_i = 0.1$s, $i = 1, 2, 3$. The weighted matrices are simply set as $Q_i = \tilde{Q}_i = \begin{bmatrix} 0.2 & 0 \\ 0 & 0.2 \end{bmatrix}$, $R_i = \tilde{R}_i = \begin{bmatrix} 0.1 & 0 \\ 0 & 0.1 \end{bmatrix}$, $i = 1, 2, 3$. According to Assumption 3, $K_1 = K_3 = [-0.8752\ -1.1245]$, $K_2 = [-0.8724\ -1.1230]$ can be calculated by LQR. In view of Lemmas 1 and 2, it is obtained that $P_1 = P_3 = \tilde{P}_1 = \tilde{P}_3 = \begin{bmatrix} 0.2915 & 0.1094 \\ 0.1094 & 0.1406 \end{bmatrix}$, $P_2 = \tilde{P}_2 = \begin{bmatrix} 0.2911 & 0.1091 \\ 0.1091 & 0.1404 \end{bmatrix}$, and $\varepsilon_i = 0.19$, $i = 1, 2, 3$. Then, from Assumption 2, $L_{f_i} = 2.5$, $i = 1, 2, 3$. According to Theorems 1–3, we can choose $\alpha_i = 0.97$ and the prediction horizon $T_i = 0.7$s, $i = 1, 2, 3$.

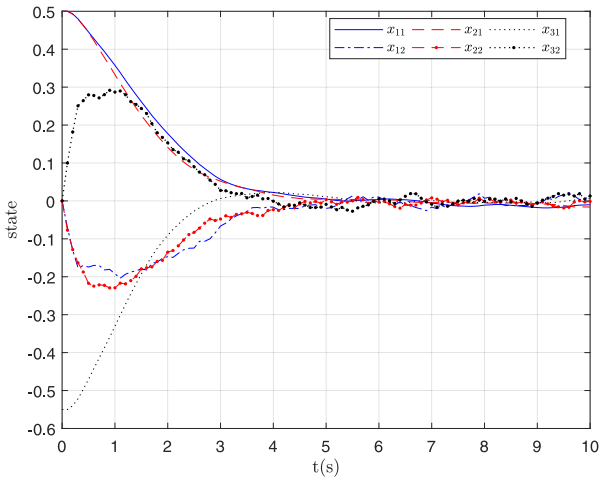

Fig. 2. The state trajectories of each cart.

The simulation results are shown in Figs. 2–5 . The state (displacement, velocity) and control input of each cart are depicted in Figs. 2–3, from which we can see that the closed-loop system is stable and the state and control input constraints are satisfied. The triggering instants of each cart under the conventional self-triggered mechanism (Eqtami et al., 2013; Hashimoto et al., 2014; Sun et al., 2019) and the proposed algorithm are shown in Figs. 4 and 5, respectively. The total number of triggering can represent the consumption of the communication resources. It can be seen that among 10 s, the total number of triggering are 12 in Fig. 4, while 6 in Fig. 5, respectively. The average computation time of conventional self-triggered mechanism and the proposed algorithm are 2.0247 s and 1.8023 s, respectively. We can see that the

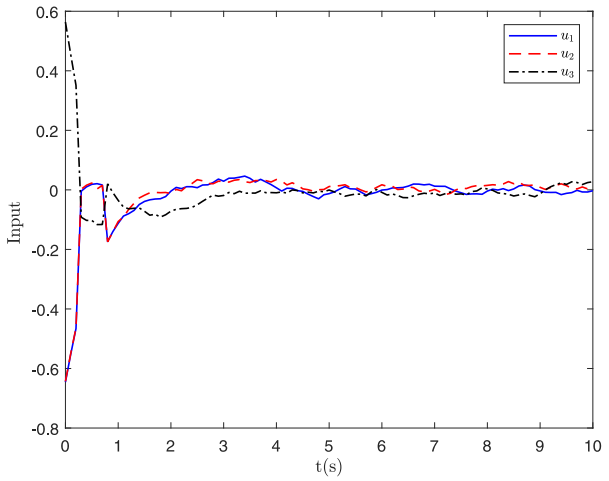

Fig. 3. The control input trajectories of each cart.

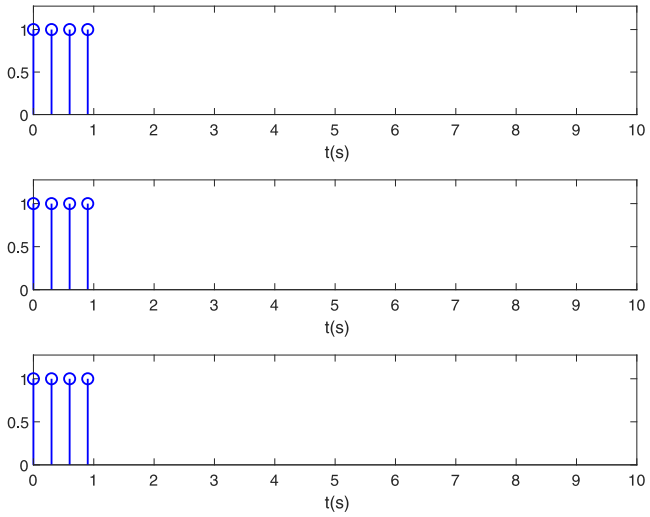

Fig. 4. Triggering instants under the conventional self-triggered mechanism.

proposed algorithm can save communication and computation resources more efficiently. To show the advantage of the proposed strategy in control performance, we compare the control performance of the proposed strategy with single nominal model strategy and the periodic triggering strategy. Define the following performance index

$$J = \sum_{i=1}^{3} \int_{0}^{10} (\|x_i(t)\|^2_{\tilde{Q}_i} + \|u_i(t)\|^2_{\tilde{R}_i}) dt$$

The value of J under the single nominal model strategy, the proposed strategy, and the periodic one are 2.6393, 2.6391, and 2.6148, respectively. Clearly, the performance obtained with the proposed strategy is better than the single nominal model strategy, and is close to the periodic one. Note that the coupling influences are weak, therefore the performance improvement is not significant. The strong coupling between subsystems will be further studied.

6. Conclusion

A rolling self-triggered DMPC strategy has been proposed for large-scale dynamically coupled systems. By implementing this strategy, the complexity of the DMPC algorithm design has been

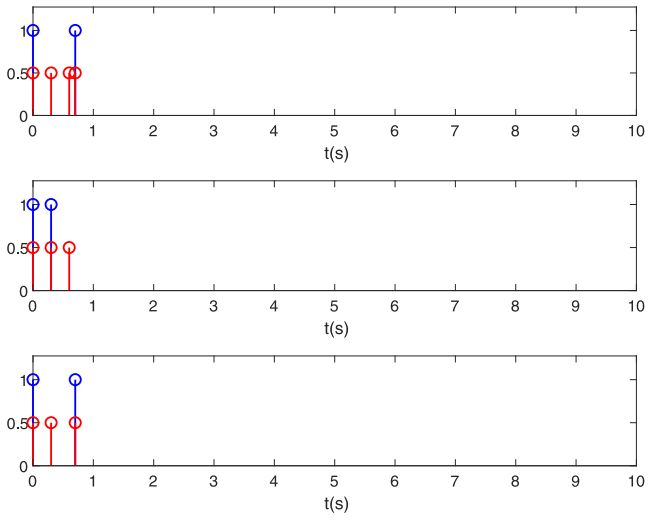

Fig. 5. Triggering instants (blue line) and sampling instants (red line) under the proposed algorithm. (For interpretation of the references to color in this figure legend, the reader is referred to the web version of this article.)

reduced while maintaining good control performance on the one hand, and on the other hand, the communication burden has been reduced significantly. We have established the sufficient conditions for the recursive feasibility of the proposed algorithm and the stability of the overall systems. Finally, simulation examples have been conducted to validate the effectiveness.

References

Alessio, A., Barcelli, D., & Bemporad, A. (2011). Decentralized model predictive control of dynamically coupled linear systems. *Journal of Process Control*, *21*(5), 705–714.

Antonelli, G. (2013). Interconnected dynamic systems: An overview on distributed control. *IEEE Control Systems Magazine*, *33*(1), 76–88.

Aswani, A., Gonzalez, H., Sastry, S. S., & Tomlin, C. (2013). Provably safe and robust learning-based model predictive control. *Automatica*, *49*(5), 1216–1226.

Berkel, F., & Liu, S. (2018). An event-triggered cooperation approach for robust distributed model predictive control. *IFAC Journal of Systems and Control*, *6*, 16–24.

Chen, H., & Allgöwer, F. (1998). A quasi-infinite horizon nonlinear model predictive control scheme with guaranteed stability. *Automatica*, *34*(10), 1205–1217.

Dai, L., Qiang, Z., Sun, Z., Zhou, T., & Xia, Y. (2020). Distributed economic MPC for dynamically coupled linear systems with uncertainties. *IEEE Transactions on Cybernetics*.

Dunbar, W. B. (2007). Distributed receding horizon control of dynamically coupled nonlinear systems. *IEEE Transactions on Automatic Control*, *52*(7), 1249–1263.

Eini, R., & Abdelwahed, S. (2019). Distributed model predictive control for intelligent traffic system. In *2019 International conference on internet of things (IThings) and IEEE green computing and communications (GreenCom) and IEEE cyber, physical and social computing (CPSCom) and IEEE smart data* (pp. 909–915). IEEE.

Eqtami, A., Heshmati-Alamdari, S., Dimarogonas, D. V., & Kyriakopoulos, K. J. (2013). A self-triggered model predictive control framework for the cooperation of distributed nonholonomic agents. In *52nd IEEE conference on decision and control* (pp. 7384–7389). IEEE.

Fu, D., Zhang, H.-T., Dutta, A., & Chen, G. (2019). A cooperative distributed model predictive control approach to supply chain management. *IEEE Transactions on Systems, Man, and Cybernetics: Systems*, *50*(12), 4894–4904.

Hanmandlu, M., & Goyal, H. (2008). Proposing a new advanced control technique for micro hydro power plants. *International Journal of Electrical Power & Energy Systems*, *30*(4), 272–282.

Hans, C. A., Braun, P., Raisch, J., Grüne, L., & Reincke-Collon, C. (2018). Hierarchical distributed model predictive control of interconnected microgrids. *IEEE Transactions on Sustainable Energy*, *10*(1), 407–416.

Hashimoto, K., Adachi, S., & Dimarogonas, D. V. (2014). Distributed aperiodic model predictive control for multi-agent systems. *IET Control Theory & Applications*, *9*(1), 10–20.

Jia, D., & Krogh, B. (2002). Min-max feedback model predictive control for distributed control with communication. In *Proceedings of the 2002 American control conference (IEEE Cat. no. CH37301), vol. 6* (pp. 4507–4512). IEEE.
Kang, Y., Wang, T., Li, P., Xu, Z., & Zhao, Y.-B. (2022). Compound event-triggered distributed MPC for coupled nonlinear systems. *IEEE Transactions on Cybernetics*.
Li, H., Yan, W., Shi, Y., & Wang, Y. (2015). Periodic event-triggering in distributed receding horizon control of nonlinear systems. *Systems & Control Letters*, *86*, 16–23.
Lin, X., Görges, D., & Weißmann, A. (2017). Simplified energy-efficient adaptive cruise control based on model predictive control. *IFAC-PapersOnLine*, *50*(1), 4794–4799.
Liu, Q., Abbas, H. S., & Velni, J. M. (2018). An LMI-based approach to distributed model predictive control design for spatially-interconnected systems. *Automatica*, *95*, 481–487.
Liu, C., Li, H., Shi, Y., & Xu, D. (2020). Distributed event-triggered model predictive control of coupled nonlinear systems. *SIAM Journal on Control and Optimization*, *58*(2), 714–734.
Liu, X., Shi, Y., & Constantinescu, D. (2014). Distributed model predictive control of constrained weakly coupled nonlinear systems. *Systems & Control Letters*, *74*, 41–49.
Ma, A., Liu, K., Zhang, Q., Liu, T., & Xia, Y. (2020). Event-triggered distributed MPC with variable prediction horizon. *IEEE Transactions on Automatic Control*.
Ma, A., Liu, K., Zhang, Q., & Xia, Y. (2020). Distributed MPC for linear discrete-time systems with disturbances and coupled states. *Systems & Control Letters*, *135*, Article 104578.
Magni, L., & Scattolini, R. (2006). Stabilizing decentralized model predictive control of nonlinear systems. *Automatica*, *42*(7), 1231–1236.
Mirzaei, A., & Ramezani, A. (2021). Cooperative optimization-based distributed model predictive control for constrained nonlinear large-scale systems with stability and feasibility guarantees. *ISA Transactions*.
Paulavičius, R., & Žilinskas, J. (2006). Analysis of different norms and corresponding Lipschitz constants for global optimization. *Technological and Economic Development of Economy*, *12*(4), 301–306.
Shalmani, R. A., Rahmani, M., & Bigdeli, N. (2020). Nash-based robust distributed model predictive control for large-scale systems. *Journal of Process Control*, *88*, 43–53.
Sun, Z., Dai, L., Liu, K., Dimarogonas, D. V., & Xia, Y. (2019). Robust self-triggered MPC with adaptive prediction horizon for perturbed nonlinear systems. *IEEE Transactions on Automatic Control*, *64*(11), 4780–4787.
Wang, T., Li, P., Kang, Y., & Zhao, Y.-B. (2021). Self-triggered model predictive control for perturbed nonlinear systems: An iterative implementation. In *2021 60th IEEE conference on decision and control* (pp. 1281–1286). IEEE.
Zhou, Y., Li, D., Xi, Y., & Gao, F. (2022). Event-triggered distributed robust model predictive control for a class of nonlinear interconnected systems. *Automatica*, *136*, Article 110039.

Tao Wang received the Ph.D. degree in control science and engineering from the University of Science and Technology of China, Hefei, China, in 2023.

He is a Lecturer with the School of Electrical and Automation Engineering, Hefei University of Technology. His research interests include networked control systems, model predictive control, power systems.

Yu Kang received the Ph.D. degree in control theory and control engineering from the University of Science and Technology of China, Hefei, China, in 2005.

From 2005 to 2007, he was a Postdoctoral Fellow with the Academy of Mathematics and Systems Science, Chinese Academy of Sciences. He is currently a Professor with the Department of Automation and the Institute of Advanced Technology, University of Science and Technology of China. His current research interests include monitoring of vehicle emissions, adaptive/robust control, variable structure control, mobile manipulator, and Markovian jump systems.

Pengfei Li received the Ph.D. degree in control science and engineering from the University of Science and Technology of China (USTC), Hefei, China, in 2020.

He is an Associate Research Fellow with the School of Information Science and Technology, USTC. His research interests include networked control systems, model predictive control, and learning based control.

Yun-Bo Zhao received his B.Sc. degree in mathematics from Shandong University, Jinan, China in 2003, M.Sc. degree in systems sciences from the Key Laboratory of Systems and Control, Chinese Academy of Sciences, Beijing, China in 2007, and Ph.D. degree in control engineering from the University of South Wales (formerly University of Glamorgan), Pontypridd, UK in 2008, respectively.

He is currently a Professor with University of Science and Technology of China, Hefei, China. He is mainly interested in AI-driven control and automation, specifically, AI-driven networked intelligent control, AI-driven human–machine autonomies and AI-driven machine gaming.

Hao Tang received the B.E. degree in industrial electrical automation from Anhui Institute of Technology, Hefei, China, in 1995, the M.E. degree in nuclear energy science and technology from the Institute of Plasma Physics, Chinese Academy of Sciences, Hefei, in 1998, and the Ph.D. degree in pattern recognition and intelligent system from the University of Science and Technology of China, Hefei, in 2002.

From 2005 to 2007, he was a Postdoctoral Researcher with The University of Tokyo, Tokyo, Japan. He is currently a Professor with the School of Electrical Engineering and Automation, Hefei University of Technology, Hefei. His current research interests include discrete-event dynamic systems, reinforcement learning, the methodology of neurodynamic programming, power system analysis, and human–machine interaction.